Room-Temperature Chemisorption and Thermal Evolution of 1,1-Dichloroethylene and Monochloroethylene on Si(111)7×7: Formation of Vinylidene and Vinylene Adspecies

Zhenhua He, Q. Li, and K. T. Leung*

Department of Chemistry University of Waterloo, Waterloo, Ontario N2L 3G1, Canada

Received: February 11, 2005; In Final Form: May 18, 2005

The room-temperature (RT) adsorption and thermal evolution of 1,1-dichloroethylene (1,1-$C_2H_2Cl_2$ or *iso*-DCE) and monochloroethylene (C_2H_3Cl or MCE) on Si(111)7×7 have been studied by vibrational electron energy loss spectroscopy and thermal desorption spectrometry (TDS). The presence of the Si−Cl stretch at 510 cm^{-1} suggests that upon adsorption *iso*-DCE dissociates via C−Cl bond breakage on the 7×7 surface to form mono-σ-bonded 1-chlorovinyl ($Cl\dot{C}{=}CH_2$) and/or di-σ-bonded vinylidene ($:C{=}CH_2$) adspecies. Upon annealing to 450 K, the 1-chlorovinyl adspecies undergoes further dechlorination to vinylidene adspecies, which may be converted to di-σ-bonded vinylene ($H\dot{C}{=}\dot{C}H$) before dehydrogenating to hydrocarbon fragments above 580 K. TDS studies reveal both molecular desorption of *iso*-DCE near 350 K and C_2H_2 fragments near 700 K, and the presence of the latter confirms the existence of the di-σ-bonded vinylene adspecies. Like the other chlorinated ethylene homologues, *iso*-DCE also exhibits TDS features of an etching product $SiCl_2$ at 800−950 K and a dehydrochlorination product HCl at 700−900 K. Unlike *iso*-DCE, MCE is found to adsorb on the 7×7 surface predominantly through a [2 + 2] cycloaddition mechanism at RT, with similar di-σ bonding structure as ethylene. The thermal evolution of MCE however follows that of *iso*-DCE, with the formation of vinylene above 580 K. Despite the lack of TDS feature attributable to HCl, weaker $SiCl_2$ TDS feature could be observed at 800−950 K. For both *iso*-DCE and MCE, strong recombinative desorption of H_2 is observed near 780 K. The differences in the Cl content among *iso*-DCE, MCE, and ethylene therefore play a key role in the RT chemisorption and thermally driven chemical processes on Si(111)7×7.

1. Introduction

The interaction of chlorinated hydrocarbons with silicon surfaces is of practical interest to the semiconductor industry because of their important role as common industrial chemicals for processing and treatment of silicon wafers.[1−4] Our group has recently conducted a series of studies on the surface chemical processes of chlorinated ethylenes on two model silicon surfaces: Si(111)7×7[5] and Si(100)2×1.[6] In particular, dechlorination appears to be a common reaction on both surfaces, and novel adstructures involving chlorinated derivatives of vinyl, vinylene, and vinylidene adspecies could be produced upon thermal excitation.[5,6] Furthermore, the stabilities of these chlorinated adspecies appear to be greatly affected by the chlorine content. In the present work, we investigate the room-temperature chemisorption and thermal evolution of 1,1-dichloroethylene (1,1-$C_2H_2Cl_2$ or *iso*-DCE) on Si(111)7×7 by vibrational electron energy loss spectroscopy (EELS) and thermal desorption spectrometry (TDS). These results are compared with those obtained for vinyl chloride or monochloroethylene (C_2H_3Cl or MCE) and ethylene (C_2H_4) to evaluate the roles of chlorine and structural symmetry in the surface chemistry of Si(111)7×7. The effects of different geometrical isomers for dichloroethylene (including *cis*-, *trans*-, and *iso*-DCE) are also of interest, and these will be presented in a follow-up work.[7] The Si(111)7×7 surface provides a wide range of different directional bonding possibilities, involving corner and center adatoms, rest atoms, dimer-row atoms, and corner-hole atoms as well as pedestal atoms as depicted in the dimer adatom stacking-fault (DAS) model.[8] In addition to the different dangling bonds at the adatoms, rest atoms, and corner-hole atoms, the Si−Si back bonds (between an adatom and a pedestal atom) have also been found to be highly reactive,[9] as, e.g., in the oxidation of Si by the formation of the Si−O−Si species.[10] An earlier study has also proposed various bonding possibilities for acetylene and ethylene involving bonding with the pedestal atom on the 7×7 surface, upon saturation of the adjacent adatom-rest-atom pairs by cycloaddition reactions.[11] The reactivities and selectivities of these different bonding sites toward chlorinated ethylenes are therefore of fundamental interest to organosilicon chemistry.

To date, only a limited amount of work on the degradation of chlorinated ethylenes catalyzed on metal surfaces has been reported,[11−18] and little is known about the interactions of these compounds with silicon. In particular, C−Cl dissociation has been observed for adsorption of chloroethylenes on Ag(111),[12] Cu(110),[16] Cu(100),[17] Pd(110),[18] and Pt(111),[19] similar to what has been observed by us on Si(111)7×7.[5] The formation of metal-stabilized carbenoid ($:C{=}CH_2$) on the surface upon adsorption of *iso*-DCE on Fe was proposed.[14,15] The formation of an analogous adspecies such as vinylidene on a surface with well-defined directional bonding, such as Si(111)7×7, would therefore be of great interest.

2. Experimental Section

The experimental apparatus and procedure used in the present work have been described in detail elsewhere.[20] Briefly, the experiments were conducted in a home-built ultrahigh vacuum system with a base pressure better than 5×10^{-11} Torr. All of

* To whom correspondence may be addressed. E-mail: tong@uwaterloo.ca.

10.1021/jp0507602 CCC: $30.25
Published on Web 07/14/2005

the EELS measurements were made with the sample held at room temperature (RT) under specular reflection scattering at 45° from the surface normal. A routine energy resolution of 12−17 meV (or 97−136 cm^{-1}) full width at half maximum with a typical count rate of 100 000 counts/s for the elastic peak could be achieved with our spectrometer operated at a 5-eV impact energy. It should be noted that the calibration and tuning of the EELS spectrometer typically limit the reproducibility of the measured peak positions to ±2 meV (or ±16 cm^{-1}) in the present work. The TDS experiments were obtained by using a differentially pumped quadrupole mass spectrometer (QMS) to monitor the ion fragments, along with a home-built programmable proportional-integral-differential temperature controller to provide a linear heating rate of 1 K s^{-1}. The TDS data have been smoothed by adjacent averaging, and the respective monotonically increasing backgrounds with increasing temperature have also been removed in order to more clearly identify the desorption features. The Si(111) sample (p-type boron-doped, 50 Ω cm, 8 × 6 mm^2, 0.5 mm thick) with a stated purity of 99.999% was purchased from Virginia Semiconductor Inc. The sample was mechanically fastened to a Ta sample plate with 0.25-mm-diameter Ta wires and could be annealed by electron bombardment from a heated tungsten filament at the backside of the sample. The Si(111) sample was cleaned by a standard procedure involving repeated cycles of Ar^+ sputtering and annealing to 1200 K until a sharp 7×7 low-energy electron diffraction (LEED) pattern was observed. The cleanliness of the 7×7 surface was further verified in situ by the lack of any detectable vibrational EELS feature attributable to unwanted contaminants, particularly the Si−C stretching mode at 800−850 cm^{-1}. Liquid *iso*-dichloroethylene (99% purity) was purchased from Sigma-Aldrich and was used (without further purification) after appropriate degassing by repeated freeze−pump−thaw cycles. The gaseous monochloroethylene (98% purity) was purchased from Matheson. The clean Si(111) sample was exposed to *iso*-DCE or MCE vapors at a typical pressure of 1 × 10^{-6} Torr by using a variable leak valve.

3. Results and Discussion

3.1. Room-Temperature Adsorption of iso-DCE and MCE on Si(111)7×7. Figure 1 compares the vibrational EELS spectra obtained for saturation exposures of *iso*-DCE, MCE, and ethylene on Si(111)7×7 at RT. The generally broader peak widths of the observed features suggest either a mixture of contributing vibrational modes in the same location or a single vibrational mode contributed from a mixture of plausible adsorption structures,[21] or both. To facilitate spectral assignments, we compare the present vibrational EELS data with the corresponding IR and Raman spectroscopic data obtained in the gas or liquid phase.[22−25] In Figure 2, we show schematic diagrams of plausible surface structures of the adspecies upon RT adsorption and their subsequent thermal evolution for *iso*-DCE and MCE on the 7×7 surface. Evidently, all three adsorbates exhibit a prominent C−H stretch feature near 2900 cm^{-1}, with the higher frequency found for *iso*-DCE (2980 cm^{-1}, Figure 1a) than MCE and ethylene (2900 cm^{-1}, parts b and c of Figure 1). A second common but considerably weaker feature at 1360 cm^{-1} can also be found. This mid-frequency feature can be assigned to the CH_2 scissoring mode, which indicates the presence of the CH_2 group in the adstructures for all three molecules. In the low-frequency region, both *iso*-DCE and MCE exhibit an EELS feature at 510 cm^{-1} that can be assigned to Si−Cl stretch (parts a and b of Figure 1), in accord with the characteristic frequency for the Si−Cl stretching mode commonly found in 467−600 cm^{-1}.[26,27] In contrast, this feature is clearly absent in the EELS spectrum of ethylene (Figure 1c). The feature at 510 cm^{-1} can therefore be used to indicate the relative Cl surface concentration and the degree of dechlorination upon adsorption.

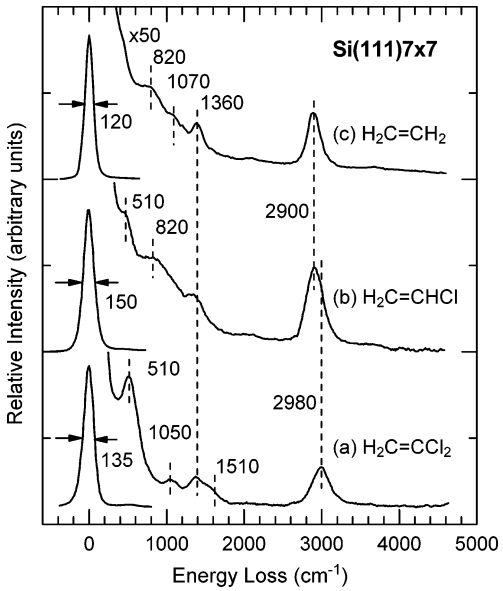

Figure 1. Vibrational EELS for saturation coverages of (a) 100 L of *iso*-dichloroethylene, (b) 1000 L of monochloroethylene, and (c) 1000 L of ethylene exposed to Si(111)7×7 at room temperature.

Figure 1 also shows that the EELS spectrum for *iso*-DCE is discernibly different from those of MCE and ethylene, both of which are found to be remarkably similar to each other. Unlike *iso*-DCE and MCE, the EELS spectrum of ethylene has been reported earlier by Yoshinobu et al.[28] and is found to be in good accord with our present measurement (Figure 1c). In addition to the prominent C−H stretch feature at 2930 cm^{-1}, several weaker features observed in the 600−1300-cm^{-1} region, including the C−C stretch at 1090 cm^{-1}, CH_2 bending modes at 1235 cm^{-1} (wag), 940 cm^{-1} (twist) and 710 cm^{-1} (rock), and Si−C stretch at 625 cm^{-1} (symmetric mode) and 795 cm^{-1} (asymmetric mode), led Yoshinobu et al. to propose that the adsorption of ethylene on Si(111)7×7 involves a [2 + 2] cycloaddition mechanism and the formation of a di-σ-bonded ethane-1,2-diyl adstructure with near-sp^3 hybridization for the C atoms.[28] The strong similarity between the EELS spectra for ethylene (Figure 1c) and MCE (Figure 1b) therefore suggests that MCE may have a predominant adstructure similar to that of ethylene on the 7×7 surface. In particular, a di-σ-bonded chloroethane-1,2-diyl adspecies (Structure IV, Figure 2b) is proposed to account for not only the C−H structure feature at a lower frequency (2900 cm^{-1}) due to C sp^3 hybridization but also the weak band at 600−1300 cm^{-1} (Figure 1b). Like ethylene, this weak band could be attributed to a mixture of several modes including C−C stretch, CH_2 bending modes and Si−C stretch, as well as the C−Cl stretch (found to be located at 705 cm^{-1} in the gas-phase spectrum).[22] However, the presence of a weak Si−Cl stretching band at 510 cm^{-1} found for MCE (Figure 1b) suggests partial dechlorination as a plausible minor adsorption channel, likely involving a mono-σ-bonded vinyl adspecies, $H\dot{C}{=}\dot{C}H_2$ (Structure V, Figure 2b). The lack of any substantial intensity near 1500 cm^{-1} commonly attributed to the C=C stretch[24] therefore confirms that the dechlorinated vinyl adspecies only plays a minor role.

Unlike MCE (Figure 1b) and ethylene (Figure 1c), *iso*-DCE exhibits a weak but well-defined feature at 1050 cm^{-1} (Figure

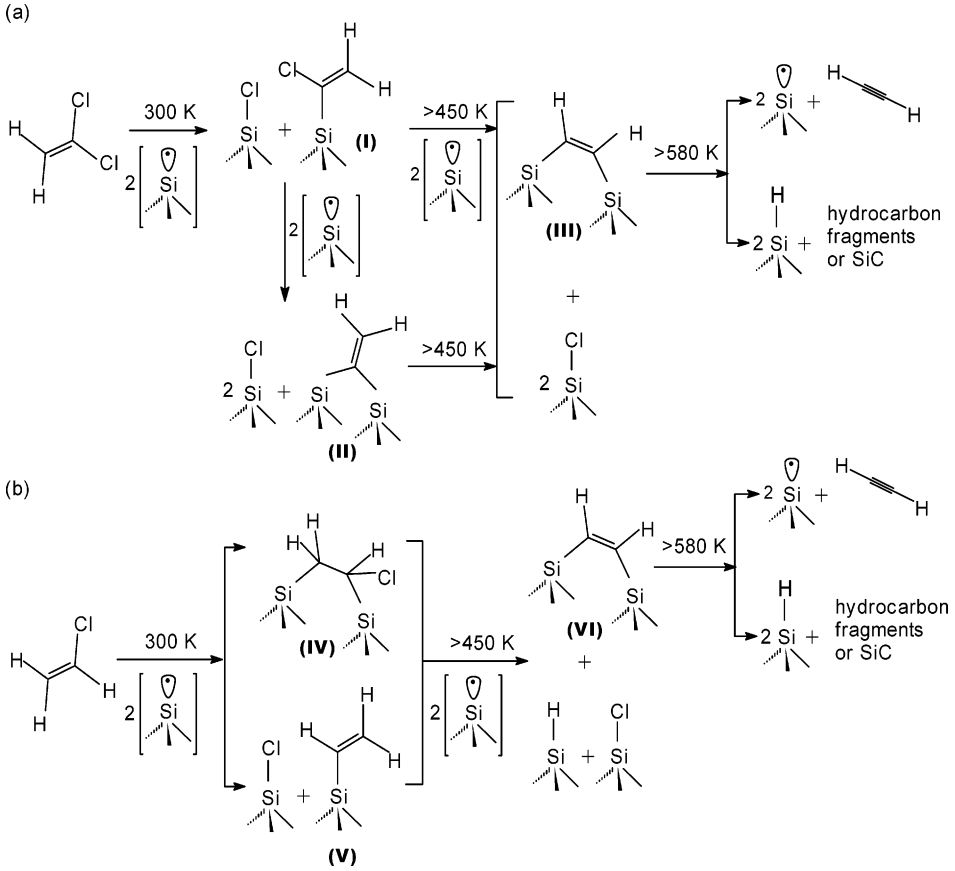

Figure 2. Schematic diagrams of plausible adsorption structures and thermal evolution products for (a) *iso*-dichloroethylene and (b) monochloroethylene exposed to Si(111)7×7 at room temperature.

1a), which can be assigned to CH_2 rocking modes in accord with the value found for the liquid phase.[24] The absence of a discernible asymmetric Si−C stretch near 795 cm^{-1} as found in ethylene (and MCE)[28] is consistent with a C sp^2 mono-σ bonding to the Si substrate, with the corresponding Si−C stretch expected below 700 cm^{-1}. The relatively well-defined shape of the feature at 1050 cm^{-1} is related to the absence of the other CH_2 bending features (twist and wag) due to the C sp^2 hybridization for mono-σ-bonded adstructures of *iso*-DCE (instead of C sp^3 hybridization as in the case of MCE and ethylene) on the 7×7 surface.[28] The blue shift of the C−H stretch feature from 2900 cm^{-1} for MCE (Figure 1b) and ethylene (Figure 1c) to 2980 cm^{-1} for *iso*-DCE (Figure 1a) is consistent with the difference in the C hybridization (between sp^3 and sp^2) involved in the respective adstructures. Furthermore, *iso*-DCE also exhibits a new feature at 1510 cm^{-1} not found in MCE and ethylene. Given that the C−C stretch in single, double, and triple C−C bonds is generally found at 950, 1600, and 2100 cm^{-1}, respectively,[24] the shoulder at 1510 cm^{-1} (Figure 1a) can therefore be assigned to C═C stretch, which again confirms the C sp^2 hybridization. Together with the strong Si−Cl stretch at 510 cm^{-1} found in the *iso*-DCE spectrum (Figure 1a) that clearly indicates dechlorination of *iso*-$C_2H_2Cl_2$ upon adsorption, the presence of the C═C stretch provides strong evidence for 1-chlorovinyl adspecies (Structure I, Figure 2a) as the most likely adstructure for *iso*-DCE, although we cannot rule out the double-dechlorinated adstructure such as vinylidene (: C═CH_2, Structure II, Figure 2a), which would require more Si dangling bonds.

It should be noted that we also collected EELS spectra for our sample pre- and postexposed to O_2 (not shown). In particular, no EELS features attributable to *iso*-DCE are observed for an oxidized Si(111) surface exposed to 20 L of *iso*-DCE. Similarly, the EELS spectrum for 20 L of *iso*-DCE exposed to Si(111) is unchanged by postexposure with 200 L of O_2, and no Si−O−Si related feature is found. These results show that dangling bonds are required for the initial adsorption of both O_2 and *iso*-DCE, and exposure of either adsorbate has the effect of passivating the surface. These results are also consistent with the conversion of the 7×7 LEED pattern for the clean surface to a 1×1 pattern for the surface exposed to either adsorbate. Furthermore, exposure of *iso*-DCE to an argon-sputtered Si(111) surface appears to produce broad features below 1200 cm^{-1}, while the prominent C−H stretch near 2980 cm^{-1} remains well defined. This EELS data (not shown) suggests that the RT adsorption of *iso*-DCE largely involves molecular adsorption with a range of (weakly) bonding configurations on the sputtered surface, in good accord with the relatively stronger molecular desorption feature at 350 K observed in the corresponding TDS experiment (not shown).

3.2. Thermal Evolution of iso-DCE and MCE on Si(111)7×7. Figures 3 and 4 show respectively the TDS profiles of selected mass fragments for 100 L of *iso*-DCE and 1000 L of MCE exposed to Si(111)7×7 at RT. For the *iso*-DCE experiments, an apparently common desorption feature at 350 K can be observed for mass 98 ($C_2H_2{}^{35}Cl^{37}Cl^+$, Figure 3g), mass 96 ($C_2H_2{}^{35}Cl_2{}^+$, corresponding to the parent mass, Figure 3f), and mass 63 ($C_2H_2{}^{37}Cl^+$, Figure 3e). Because their corresponding peak intensity ratios for these TDS features are found to be in good accord with the respective ratios of the cracking pattern of *iso*-DCE,[29] the detected mass fragments could be attributed to dissociation of molecularly desorbed *iso*-DCE in the ionizer of the QMS. Similarly, the TDS profile of the parent mass for MCE, mass 62 ($C_2H_2{}^{35}Cl_2{}^+$), also exhibits a desorption peak

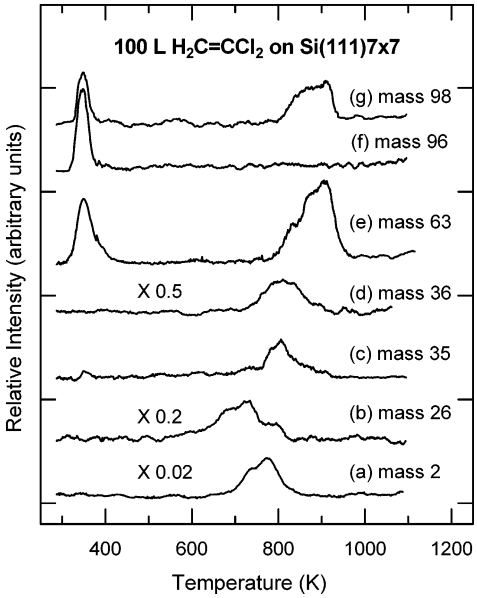

Figure 3. Thermal desorption profiles of (a) mass 2 (H_2^+), (b) mass 26 ($C_2H_2^+$), (c) mass 35 (Cl^+), (d) mass 36 (HCl^+), (e) mass 63 ($C_2H_2{}^{37}Cl^+$ or $Si^{35}Cl^+$), (f) mass 96 ($C_2H_2{}^{35}Cl_2^+$), and (g) mass 98 ($C_2H_2{}^{35}Cl^{37}Cl^+$ or $Si^{35}Cl_2^+$) for 100 L of *iso*-dichloroethylene exposed to Si(100)7×7 at room temperature.

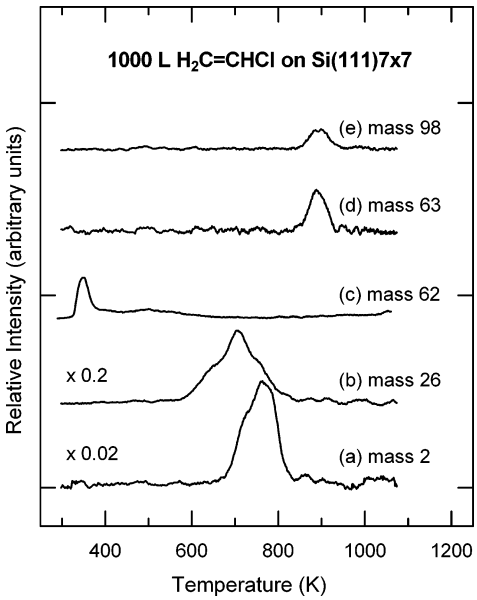

Figure 4. Thermal desorption profiles of (a) mass 2 (H_2^+), (b) mass 26 ($C_2H_2^+$), (c) mass 62 ($C_2H_3{}^{35}Cl^+$), (d) mass 63 ($Si^{35}Cl^+$), and (e) mass 98 ($Si^{35}Cl_2^+$) for 1000 L of monochloroethylene exposed to Si(100)7×7 at room temperature.

near 350 K (Figure 4c). To ensure that the desorbed species indeed come from the Si sample instead of the sample holder, we positioned the front face of the sample as close as possible (within 1 mm) to the entrance of the differentially pumped housing of the QMS for the TDS experiments. Such an arrangement has been found to be effective in lowering the background and in preventing desorbed species in the surroundings from entering the ionizer region. Moreover, we conducted the TDS experiments for *iso*-DCE on a Ni(110) surface using the same sample holder setup, and we did not observe the same desorption products, which affirms that the desorbed species indeed come from the Si sample and not the sample holder. The relatively low temperature of the desorption maximum for the parent mass of *iso*-DCE suggests that the molecularly desorbed species originate from the as-deposited (intact) molecules and not from recombinative desorption of adsorbed dissociated fragments, which would require a higher desorption temperature. However, unlike MCE (Structure IV, Figure 2b), the bonding structure of the molecularly adsorbed *iso*-DCE is unclear. One bonding possibility may involve weak dative covalent bonding between the Cl atoms and the substrate Si atoms as a result of the inductive effect of the Cl atoms.

For *iso*-DCE (and MCE), the respective TDS profiles of masses 98 and 63 (mass 62) also exhibit a broad feature located at 800−950 K, which could be attributed to desorption of $SiCl_2^+$ and $SiCl^+$, respectively (Figures 3 and 4). An earlier chemisorption study of $SiCl_4$ and SiH_2Cl_2 on Si(100) and Si(111) surfaces has suggested that these higher-temperature TDS features may correspond to disproportionation of two monochloride species.[30] The nearly identical profile shapes of these higher-temperature features of masses 98 and 63 (with an intensity ratio of 1.8 for mass 63 to mass 98) for *iso*-DCE also indicate that they originate from the same desorption product. Because $SiCl_2^+$ (mass 98) and $SiCl^+$ (mass 63) are found to be in comparable amounts from electron impact studies of gaseous $SiCl_2$,[31,32] the parent desorption species is likely $SiCl_2$. In our TDS experiments for *iso*-DCE and MCE, we have also monitored but found no mass 133, corresponding to $SiCl_3^+$ of the heavier etching product $SiCl_4$, confirming $SiCl_2$ as the main etching product. Furthermore, two broad additional desorption features of mass 36 (HCl^+, Figure 3d) and mass 35 (Cl^+, Figure 3c) at 700−900 K are also observed for *iso*-DCE, which indicates recombinative desorption of HCl upon thermal evolution. In contrast, no disernible TDS features of mass 36 (HCl^+) and mass 35 (Cl^+) are detected for MCE, which confirms our EELS observation that the relative Cl surface concentration for MCE (Figure 1b) is considerably less than that of *iso*-DCE (Figure 1a) as indicated by the relative intensities of the respective Si−Cl stretch features at 510 cm^{-1}. For both *iso*-DCE (Figure 3a) and MCE (Figure 4a), an intense broad feature of mass 2 (H_2^+) is also observed at 650−850 K (with the desorption maximum at 780 K), in good accord with the recombinative H_2 desorption from Si monohydrides (with the desorption maximum commonly observed at 770−810 K).[33,34] Given the lower Cl concentration found for MCE adsorption, the faster kinetics of recombinative desorption for H_2 than HCl[30,31,32] may explain the absence of any discernible features of mass 36 (HCl^+) and mass 35 (Cl^+) for MCE. In addition, both *iso*-DCE and MCE also exhibit a broad TDS feature of mass 26 ($C_2H_2^+$) at 550−820 K (with the desorption maximum near 710 K, Figures 3b and 4b), in good accord with acetylene desorption from di-σ-bonded vinylene (HĊ=ĊH) on a Si surface that is generally observed with a desorption maximum at 750 K.[35] It should be noted that we also monitored but found no desorption feature for mass 27, which belongs to the cracking pattern of and could therefore be used as a signature for ethylene (the parent mass of ethylene, mass 28, was not monitored due to the high background). The evolution of the mass-26 TDS feature therefore indicates the plausible formation of di-σ-bonded vinylene upon annealing of adsorbed *iso*-DCE and MCE on Si(111)7×7 (Figure 2).

To further investigate the nature of the surface products during thermal evolution, we record EELS spectra for a 100-L exposure of DCE (shown in Figure 5) and a 200-L exposure of MCE (shown in Figure 6) to the 7×7 surface upon annealing the respective samples to different temperatures. In particular, upon annealing the *iso*-DCE/Si(111)7×7 sample to 450 K, we observe discernible increase in the intensity of the Si−Cl stretch at 510

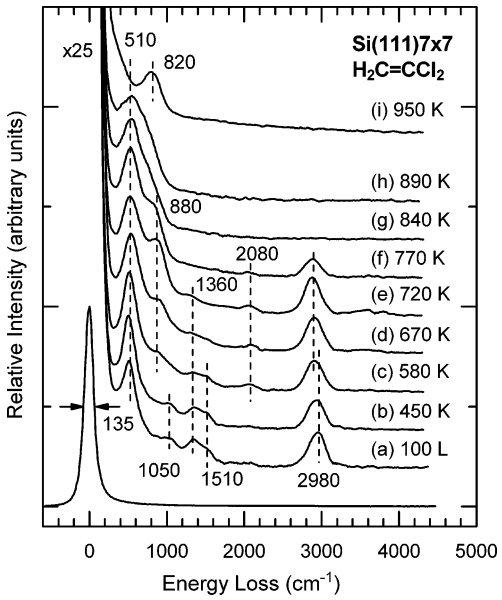

Figure 5. Vibrational EELS for 100 L of *iso*-dichloroethylene exposed to (a) Si(111)7×7 at room temperature and upon annealing to (b) 450 K, (c) 580 K, (d) 670 K, (e) 720 K, (f) 770 K, (g) 840 K, (h) 890 K, and (i) 950 K.

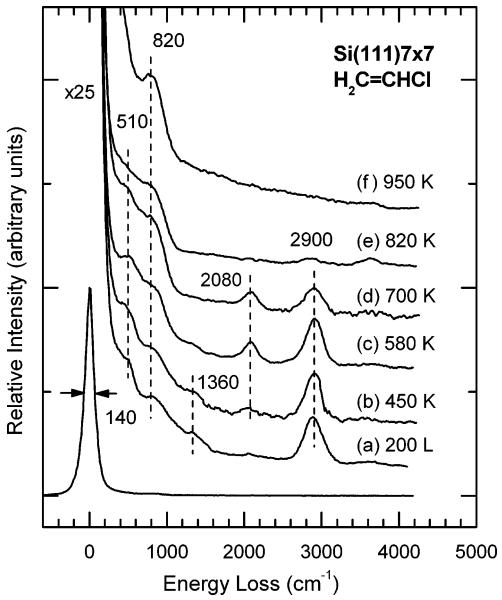

Figure 6. Vibrational EELS for 200 L of monochloroethylene exposed to (a) Si(111)7×7 at room temperature and upon annealing to (b) 450 K, (c) 580 K, (d) 700 K, (e) 820 K, and (f) 950 K.

cm^{-1}, along with minor weakening of the CH_2 scissoring feature at 1360 cm^{-1} and of the prominent C—H stretch feature at 2980 cm^{-1} (Figure 5b). Further enhancement in the Si—Cl stretch at 510 cm^{-1} and continual reduction in the CH_2 scissoring mode at 1360 cm^{-1} are found upon further annealing the sample to 580 K, while the C—H stretch feature at 2980 cm^{-1} appears to undergo a red shift to 2900 cm^{-1} (Figure 5c). These intensity changes are consistent with thermal dechlorination of the 1-chlorovinyl adspecies ($Cl\dot{C}{=}\dot{C}H_2$, Structure I, Figure 2a) to vinylidene ($:C{=}CH_2$, Structure II, Figure 2a) and/or vinylene ($H\dot{C}{=}\dot{C}H$, Structure III, Figure 2a). Furthermore, the nearly complete reductions of the weak CH_2 rocking mode at 1050 cm^{-1} and of the C=C stretch at 1510 cm^{-1} follow that of the CH_2 scissoring mode at 1360 cm^{-1}, which are consistent with the conversion of the adstructures to vinylene above 450 K (Figure 2a). It should be noted that in addition to the change in the C hybridization from sp^2 to sp^3, the red shift in the C—H stretch feature could also be caused by a change in the immediate chemical environment (i.e., the attached ligands or groups) of the host C atom. In particular, the C—H bond in the ($=C<^{H}_{Si}$) group as in vinylene (Structure III, Figure 2a) is slightly weaker than that in the ($=C<^{H}_{H}$) group as in 1-chlorovinyl adspecies (Structure I, Figure 2a) due to the lower electronegativity of Si (1.8 in the Pauling scale) relative to H (2.1) and C (2.5).[36] The observed red shift in the C—H stretch at 2980 cm^{-1} (Figure 5b) to 2900 cm^{-1} (Figure 5c) upon annealing the sample to 580 K is therefore consistent with our proposed thermal evolution pathway shown in Figure 2a.

From 580 K (Figure 5c) to 720 K (Figure 5e), the intensity of the red-shifted C—H stretch feature at 2900 cm^{-1} remains relatively stable but undergoes considerable reduction leading to total extinction upon further annealing to 840 K (Figure 5g). A new feature at 820 cm^{-1} attributable to Si—C stretch emerges above 840 K (Figure 5g), and it becomes a prominent well-defined peak upon further annealing to 950 K (Figure 5i). These spectral changes in the higher temperature regime are in good accord with the breakdown of the hydrocarbon fragment adspecies and the formation of SiC above 840 K. In addition, two new features at 880 and 2080 cm^{-1} attributable primarily to SiH_2 scissoring mode and Si—H stretch, respectively,[21] are found to emerge at an annealing temperature of 580 K (Figure 5c), which marks the onset of dehydrogenation of the adspecies and the formation of hydrocarbon fragments, likely in the form of CCH radicals with the characteristic CH bending modes at 850−900 cm^{-1} [16] (Figure 5a). The formation of the dihydrides is consistent with the majority of the active sites (i.e., with unoccupied dangling bonds) having already been occupied by dissociated Cl atoms and hydrocarbon fragments at this temperature. The intensities of the features at 880 and 2080 cm^{-1} appear to reach a maximum near 720 K (Figure 5e) and completely disappear above 770 K (Figure 5f), in good accord with the TDS profile of recombinative H_2 desorption at 650−850 K (Figure 3a). Upon reaching maximum intensity at an annealing temperature of 580 K, the Si—Cl stretch at 510 cm^{-1} is found to gradually weaken upon further annealing to 950 K (Figure 5i), which is in accord with the reduction in the relative Cl surface concentration due to the desorption of $SiCl_2$ at 800−950 K and HCl at 700−900 K (Figure 3).

Similar observations for the thermal evolution of the Si—Cl stretch at 510 cm^{-1}, the CH_2 scissoring feature at 1360 cm^{-1}, and the prominent C—H stretch feature at 2900 cm^{-1} can be made for a 200 L exposure of MCE (Figure 6) as those for *iso*-DCE on Si(111)7×7 at RT (Figure 5). In particular, a minor increase in the intensity of the Si—Cl stretch at 510 cm^{-1}, and minor decreases in those of the CH_2 scissoring feature at 1360 cm^{-1} and the prominent C—H stretch feature at 2900 cm^{-1} are observed, upon annealing the MCE sample to 580 K (Figure 6c). These intensity changes are again in good accord with the proposed continued breakage of the C—Cl bonds and the transfer of the Cl atoms onto the surface above 450 K (Figure 2b). The intensity reductions in the CH_2 scissoring feature at 1360 cm^{-1} and the C—H stretch feature at 2900 cm^{-1} observed in this annealing temperature range appear to coordinate with a concomitant increase in the intensity of the Si—H stretch at 2080 cm^{-1}. Such a correlation strongly suggests that H abstraction of the predominant di-σ-bonded chlorovinylene adspecies ($HCl\dot{C}{=}\dot{C}H_2$, Structure IV, Figure 2b) by the substrate Si atoms upon annealing the sample to 580 K. It is of interest to note that, unlike the C—H stretch feature for the *iso*-DCE adstructure that is found to undergo a red shift from 2980 to 2900 cm^{-1}

upon annealing to 580 K (Figure 5c), the corresponding C—H stretch in the proposed vinylene product (HĊ═ĊH, Structure VI, Figure 2b) is expected to be similar to that in chloroethane-1,2-diyl adspecies. The absence of the red shift in the C—H stretch feature at 2900 cm^{-1} is therefore consistent with the proposed thermal evolution pathway (Figure 2b). Upon further annealing of the sample to 820 K (Figure 6e), the C—H stretch feature at 2900 cm^{-1} is found to be completely diminished, which indicates total thermal breakdown of the vinylene adspecies into SiC and/or hydrocarbon fragments. The Si—Cl stretch feature at 510 cm^{-1} is found to gradually diminish over the annealing temperature of 700−820 K (parts d and e of Figure 6), which is in good accord with the desorption of the etching products $SiCl_2$ over 800−950 K found for the masses 63 and 98 TDS profiles (Figure 4). Furthermore, a similar reduction in the intensity of the Si—H stretch at 2080 cm^{-1} is also observed at 700−820 K, which is in good accord with the desorption of H_2 at 700−850 K (Figure 4d). Moreover, although the intensity of the weak band at 600−1300 cm^{-1} appears to be relatively stable upon annealing to 580 K, the nature and composition of this band (which has been previously attributed to a mixture of C—C stretch, CH_2 bending modes, and Si—C stretch as well as the C—Cl stretch) may undergo complex changes. This band emerges into a well-defined Si—C stretch feature at 820 cm^{-1} upon further annealing to 950 K (Figure 6f), which can be attributed to the decomposition of the adspecies to SiC adspecies (and/or other hydrocarbon fragments) at these higher temperatures.

3.3. Thermal Evolution and Feasibility of Vinylidene and Vinylene on Si(111)7×7. The thermal evolution of the adspecies as illustrated by the respective temperature-dependent EELS spectra are therefore found to be very similar for both *iso*-DCE (Figure 5) and MCE (Figure 6). One notable difference is the onset of the Si—H stretch (at 2080 cm^{-1}) at 450 K for MCE, in contrast to the higher-temperature onset (580 K) for *iso*-DCE, which suggests that the C—H bonds are generally stronger than C—Cl bonds in the adspecies of *iso*-DCE in this temperature range. Above 580 K, both dechlorination and dehydrogenation are found to occur for the adspecies of both MCE and *iso*-DCE. Furthermore, the removal channels of Cl as $SiCl_2$ and of H as H_2 from the surface are also found to be similar for both adsorbates (although our EELS data cannot be used to implicate the HCl recombinative desorption channel). To better identify the plausible decomposition products, we compare our results with the previous studies of the decomposition of acetylene and ethylene on Si(100) and Si(111) surfaces.[37,38] In particular, acetylene has been hypothesized to adsorb on the Si surfaces as a di-σ-bonded vinylene adspecies (similar to, e.g., Structure III, Figure 2a), which could dehydrogenate to form hydrocarbon complexes with one and/or two C atoms and eventually SiC.[38] The corresponding EELS spectrum reported by the same group[39] does not reveal any C═C stretching feature at 1510 cm^{-1}. The lack of any discernible intensity for the latter feature found by Yoshinobu et al. is consistent with the near-surface-parallel orientation of the C═C bond of the vinylene adspecies. In the present case of *iso*-DCE adsorption on Si(111)7×7, we propose the thermal evolution of the 1-chlorovinyl adspecies (Structure I, Figure 2a) and a novel vinylidene adspecies (: C═CH_2, Structure II, Figure 2a) to vinylene (HĊ═ĊH, Structure III, Figure 2a) above 450 K. The persistent presence of notable intensity of the C═C stretch feature at 1510 cm^{-1}, together with the continued enhancement of the Si—Cl stretch at 510 cm^{-1}, with increasing annealing temperature up to 580 K (Figure 5c) therefore not only supports the proposed thermal dechlorination pathway of 1-chlorovinyl adspecies to vinylidene but also illustrates the remarkable thermal stability of the vinylidene adspecies. At 580 K, the increase in the intensity of the Si—H stretching mode near 2080 cm^{-1} suggests that partial decomposition of the vinylidene adspecies likely to hydrocarbon fragments may occur. It is also of interest to note that the evolution of *iso*-DCE to vinylene adspecies appears to continue at a higher temperature (580 K) than the evolution of trichloroethylene to chlorovinylene adspecies (400 K) as observed in our recent work,[40] which is in accord with the presence of an additional reaction step involved in the H rearrangement in the former case. Furthermore, the considerably smaller intensity of the Si—H stretch feature at 2080 cm^{-1} relative to the C—H stretch at 2900 cm^{-1} for *iso*-DCE (Figure 5) than that for MCE (Figure 6) during the thermal evolution suggests that H abstraction from the hydrocarbon fragments is likely inhibited by the presence of a larger amount of dissociated Cl atoms occupying the active surface sites in the case of *iso*-DCE. As the *iso*-DCE sample is annealed above 580 K, both vinylidene and vinylene may evolve into different hydrocarbon fragments, including a "tetra-σ-bonded" ethylylidyne-like (: Ċ—$\dot{C}H_2$) adspecies similar to the intermediate proposed for ethylene adsorption on Pt(110)[41] and Pt(311)[42] and/or a "tri-σ-bonded" acetylide (: C═ĊH) adspecies. In the case of MCE, there is no direct evidence for thermal evolution to vinylene (Structure VI, Figure 2b) above 450 K due to the absence of any C═C stretch feature at 1510 cm^{-1} as a result of the near-surface-parallel orientation of the C═C bond. However, the TDS feature of mass 26 at 700 K (Figure 4b) indicates the formation of acetylene, which suggests the formation of vinylene type adspecies (i.e., with a C═C double bond). The formation of vinylene from the di-σ-bonded chloroethane-1,2-diyl (Structure IV, Figure 2b) above 450 K for MCE is in marked contrast to the thermal evolution of ethylene, for which the di-σ-bonded ethane-1,2-diyl adspecies is found to break down into CH_2 and CH fragments predominantly and eventually to SiC.[37] This difference could be attributed to the presence of the Cl atom in the chloroethane-1,2-diyl adspecies, which favors a 1,2-elimination (dehydrohalogenation) reaction pathway. The observed spectral changes are consistent with our proposed thermal evolution models for the two molecules (Figure 2).

To further investigate the feasibility of the formation of vinylidene and vinylene on the 7×7 surface, we performed ab initio density functional calculations for selected adsorption structures of *iso*-DCE, MCE, and ethylene on the surface of a Si_9H_{12} cluster used for simulating part of the Si(111)7×7 surface.[43] The hybrid functionals consisting of Becke's three-parameter nonlocal exchange functional and the correlation functional of Lee−Yang−Parr (B3LYP)[44] along with the 6-31G(d) basis set were employed in all our calculations using the Gaussian 03 program.[45] The Si_9H_{12} cluster was constructed to provide a small section of the 7×7 surface that contains a corner adatom and a neighboring rest atom, using the geometrical parameters for the Si atoms deduced from the LEED data of Tong et al.[46] In the DAS model of the 7×7 surface,[8] the separation between an adatom and a restatom and that between an adatom and a pedestal atom are 4.6 and 2.4 Å, respectively.[46] Following the approaches used by Petsalakis et al.[47] and Wang et al.,[43] we first optimize the positions of the H atoms used to cap the cluster at the boundaries with the nine Si atoms frozen at the Cartesian coordinates reported by Tong et al.[46] The optimized positions of the H atoms are then frozen to provide an effective cage to maintain the structure of the model surface for the subsequent calculations, for which only the

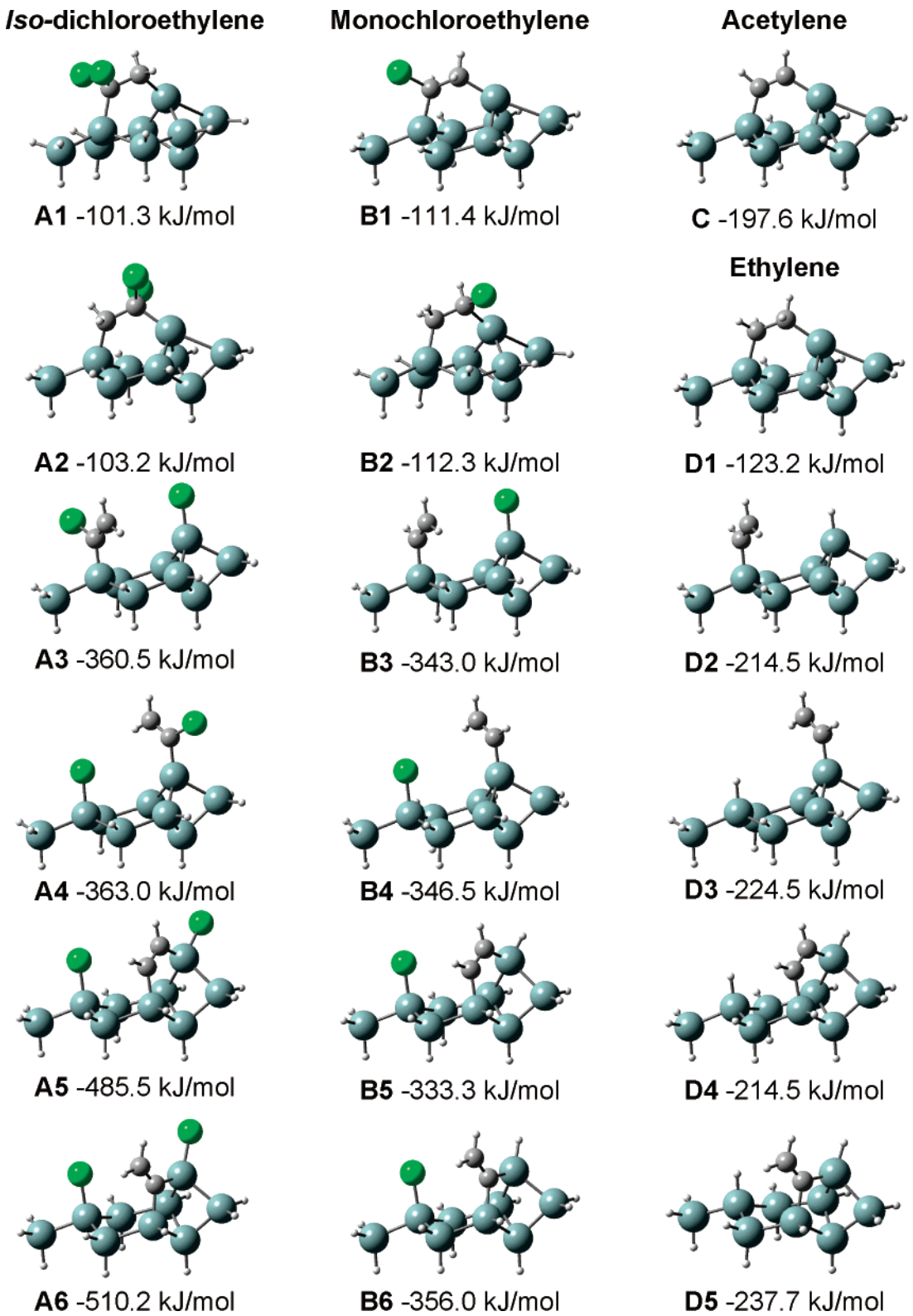

Figure 7. Schematic diagrams of the adsorption geometries, with the corresponding adsorption energies ΔH obtained by a density functional calculation involving B3LYP/6-31-G(d) for (A) *iso*-dichloroethylene, (B) monochloroethylene, (C) acetylene, and (D) ethylene on a model surface of Si_9H_{12}.

positions of the nine Si atoms and the atoms in the adsorbate are allowed to be optimized. It is important to note that the present calculation is only intended to illustrate some of the plausible structures in the proposed thermal evolution pathways shown in Figure 2. More extensive calculations that cover many other combinations of different bonding sites on the 7×7 surface are beyond the scope of the present study and should be considered in future computational work. Improved calculations involving a larger basis set, however, are not expected to significantly change the general observations inferred from the present calculation.

Figure 7 shows some of the plausible adstructures involving di-σ-bonded [2 + 2] cycloaddition species (top two rows), mono-σ-bonded dissociated products (middle two rows), and

double-dissociation products involving di-σ bonding into the back bond (bottom two rows). Except for the double-dissociation products, different conformer structures involving the different arrangements of the adspecies on the adatom and rest atom for the former adstructures are also indicated. The corresponding enthalpy changes with zero-point energy corrections, ΔH, for the adsorption/dissociation process are included in the Figure. Evidently, the ΔH values obtained for the vinylidene adspecies di-σ bonded to the adatom and the pedestal atom are the most negative ones for *iso*-DCE, MCE, and ethylene (A6, B6, D5, Figure 7), which suggests that vinylidene is physically viable through the breakage of the back-bond between the adatom and the pedestal atom and the particular arrangement appears to give the most thermodynamically stable adstructure. The ΔH values for the respective vinylene adspecies involving similar insertion into the back bond are slightly less negative (A5, B5, D4, Figure 7) than those for the corresponding vinylidene adspecies, indicating that the insertion of vinylene between the adatom and pedestal atom is nearly as thermodynamically stable as that for vinylidene. It is of interest to note that the ΔH values obtained for vinylene di-σ bonded to the adatom and restatom (averaged over the conformer configurations) are found to be more negative than those involving insertion into the back bond by 24.1 kJ mol^{-1} for *iso*-DCE (-509.6 kJ mol^{-1}), 31.7 kJ mol^{-1} for MCE (-365.0 kJ mol^{-1}), and 28.8 kJ mol^{-1} for ethylene (-243.3 kJ mol^{-1}) (not shown), which therefore suggests that the adsorption of vinylene, unlike vinylidene, favors this arrangement and not the scission of the back bond. Indeed, the vinylene in this adsorption configuration (not shown) is almost as stable as that for vinylidene for *iso*-DCE (-510.2 kJ mol^{-1}) but more stable than vinylidene for MCE (-356.0 kJ mol^{-1}) and ethylene (-237.7 kJ mol^{-1}) (Figure 7). This difference is likely due to the compatibility of the physical separations among different surface sites and the dimensions of the adspecies. By use of a typical Si$-$C bond length of 1.9 Å[48] and a bond angle between C$=$C and Si$-$C of 121°, the required separation for the two Si atoms is estimated to be 3.3 Å, which is more compatible with the larger Si$-$Si separation between the adatom and the rest atom (4.6 Å) instead of the smaller separation between the adatom and the pedestal atom (2.4 Å) that would require breakage of the back bond.[11,49] Furthermore, the two conformations of the mono-σ-bonded chlorovinyl adspecies for *iso*-DCE (A3, A4, Figure 7) and vinyl adspecies for MCE and ethylene (B3, B4, D2, D3, Figure 7) and their corresponding dissociated atoms are found to exhibit ΔH values that are generally less negative than those of their respective vinylidene and vinylene adstructures. They are however more negative than those for their [2 + 2] cycloaddition adstructures (A1, A2, B1, B2, D1, Figure 7). The magnitudes of the energy differences among different ΔH values obtained for the di-σ-bonded molecular adstructures, mono-σ-bonded dissociated chlorovinyl and vinyl adstructures, and the double-dissociation adstructures involving di-σ bonding into the back-bond (vinylidene and vinylene) are evidently related to the energy balances involved in the breakage of the C$-$Cl (with a typical bond energy ΔH_B of 339 kJ mol^{-1}) and C$-$H bonds (ΔH_B = 414 kJ mol^{-1}) and the formation of the Si$-$Cl (ΔH_B = 377 kJ mol^{-1}), Si$-$C (ΔH_B = 347 kJ mol^{-1}), and Si$-$H bonds (ΔH_B = 314 kJ mol^{-1}).[1,50,51] The changes in the ΔH values are consistent with our proposal that the adspecies resulting from dechlorination are more thermodynamically favorable than the molecularly adsorbed adstructures, particularly for *iso*-DCE. However, although the calculated ΔH values for all the adstructures shown in Figure 7 are negative, the present calculations have not considered kinetics effect. The present results should therefore only be used to indicate their thermodynamic feasibility. For example, despite its least negative ΔH value, the [2 + 2] cycloaddition product is generally accepted to be the preferred adstructure for ethylene on Si(111)7×7 (D1, Figure 7).[28] For comparison, we also show the [2 + 2] cycloaddition adstructure for acetylene (C, Figure 7). In the case of the adsorption of ethylene (and MCE) on the 7×7 surface, kinetic effects therefore play a predominant role. For *iso*-DCE, our EELS and TDS data are more consistent with the proposed dissociation surface products, which suggests that the presence of their respective adstructures is more critically controlled by their thermodynamic stabilities. It should be noted that the present calculations also have not taken into consideration of adsorption on defect sites, which could be plausible given the weak intensities of some of the spectral features. More elaborate calculations will be needed to further clarify the details of these local adsorption geometries.

4. Summary

In the present work, we investigate the RT adsorption of chlorinated derivatives of ethylene and their thermally driven surface chemistries on Si(111)7×7 by comparing the EELS and TDS data of ethylene, MCE, and *iso*-DCE. In particular, MCE, like ethylene, is found to adsorb on the 7×7 surface predominantly intact as di-σ-bonded chloroethane-1,2-diyl adspecies (Structure IV, Figure 2b). The formation of vinyl adspecies (Structure V, Figure 2b) through dissociative dechlorination is also observed as a minor adsorption channel. In contrast, the primary RT adsorption channel for *iso*-DCE on Si(111)7×7 is dissociative single- and double-dechlorination to chlorovinyl (Structure I, Figure 2a) and vinylidene adspecies (Structure II, Figure 2a), respectively. The presence of a weak molecular desorption feature at 350 K for both *iso*-DCE and MCE suggests that molecular adsorption involving dative Cl bonding (likely as a precursor state to other adstructures) also plays a minor role. The presence of two Cl atoms in *iso*-DCE instead of just one Cl in MCE therefore has a dramatic effect on the adsorption on the 7×7 surface at RT. Indeed, like the cis and trans isomers of DCE[5] and the heavier homologues including trichloroethylene and tetrachloroethylene,[40] dissociative adsorption via dechlorination appears to be the preferred channel for *iso*-DCE instead of the [2 + 2] cycloaddition pathways found in the case of MCE and ethylene. The formation of the novel vinylidene adspecies for *iso*-DCE has been supported by the persistence of the C$=$C stretch feature at 1510 cm^{-1} with increasing annealing temperature up to 580 K, together with the thermal evolution behavior of other EELS features. Our DFT calculation of model adstructures also demonstrates vinylidene as the more thermodynamically stable adspecies than vinylene and chlorovinyl adspecies for *iso*-DCE.

There are however greater similarities found in the subsequent thermal evolution of the adstructures for both MCE and *iso*-DCE. In particular, the formation of vinylene (Structure III and VI, Figure 2) by further dechlorination above 450 K and of the hydrocarbon fragments including an ethylylidyne-like (:$\dot{C}-\dot{C}H_2$) adspecies and/or an acetylide (:$C=\dot{C}H$) adspecies above 580 K are found to be plausible thermal decomposition pathways common to both adsorbates. Recombinative desorption of H_2 near 780 K and the formation of the etching product $SiCl_2$ at 800$-$950 K are also observed for both MCE and *iso*-DCE. For *iso*-DCE, additional recombinative desorption of HCl at 700$-$900 K is also found, likely due to the ready availability of dissociated Cl atoms. Furthermore, the desorption of acetylene near 700 K is observed for both MCE and *iso*-DCE, which

supports our hypothesis that the di-σ-bonded vinylene is a feasible intermediate adspecies. Further annealing the sample to above 950 K eventually converts all the remaining adspecies to SiC. The differences in the molecular structures of chlorinated ethylenes with different degrees of chlorination therefore produce dramatic effects on the formation of various novel adstructures on Si(111)7×7 at RT, many of which are found to follow similar thermal evolution pathways.

Acknowledgment. This work was supported by the Natural Sciences and Engineering Research Council of Canada.

References and Notes

(1) Buriak, J. M. *Chem. Rev.* **2002**, *102*, 1271.
(2) Lifshits, V. G.; Saramin, A. A.; Zotov, A. V. *Surface Phases on Silicon*; Wiley: New York 1994.
(3) Kuster, R.; Christmann, K. *Ber. Bunsen−Ges. Phys. Chem.* **1997**, *101*, 1799.
(4) Lagendijk, A.; Debusk, D. K. U.S. Patent 5599425, 1997.
(5) He, Z. H.; Yang, X.; Zhou, X. J.; Leung, K. T. *Surf. Sci.* **2003**, *547*, L840.
(6) Zhou, X. J.; Li, Q.; He, Z. H.; Yang, X.; Leung, K. T. *Surf. Sci.* **2003**, *543*, L668.
(7) He, Z. H.; Leung, K. T. *Surf. Sci.* **2005**, submitted.
(8) Takayanagi, K.; Tanishiro, T.; Takahashi, S.; Takashashi, M. *J. Vac. Sci. Technol. A* **1985**, *3*, 1502.
(9) Boland, J. J.; Villarrubia, J. S. *Science* **1990**, *248*, 838.
(10) Ibach, H.; Bruchmann, H. D.; Wagner, H. *Appl. Phys. A* **1982**, *29*, 113.
(11) Rochet, F.; Dufour, G.; Prieto, P.; Sirotti, F.; Stedile, F. C. *Phys. Rev. B* **1998**, *57*, 6738.
(12) Pursell, D. P.; Bocquet, M.-L.; Vohs, J. M.; Dai, H.-L. *Surf. Sci.* **2003**, *522*, 90, and reference therein.
(13) Lien, H.-L.; Zhang, W.-X. *Colloids Surf., A* **2001**, *191*, 97.
(14) Arnold, W. A.; Roberts, A. L. *Environ. Sci. Technol.* **2000**, *34*, 1794.
(15) Stang, P. *J. Chem. Rev.* **1978**, *78*, 383.
(16) Laroze, S. C.; Haq, S.; Raval, R.; Jugnet, Y.; Bertolini, J. C. *Surf. Sci.* **1999**, *435*, 193.
(17) Yang, M. X.; Kash, P. W.; Sun, D.-H.; Flynn, G. W.; Bent, B. E.; Holbrook, M. T.; Bare, S. R.; Fischer, D. A.; Gland, J. L. *Surf. Sci.* **1997**, *380*, 151.
(18) Bloxham, L. H.; Haq, S.; Mitchell, C.; Raval, R. *Surf. Sci.* **2001**, *489*, 1.
(19) Grassian, V. H.; Pimentel, G. C. *J. Chem. Phys.* **1988**, *88*, 4478.
(20) Hu, D. Q. Ph.D. Thesis, University of Waterloo, Waterloo, 1993.
(21) Ibach, H.; Mills, D. L. *Electron energy Loss Spectroscopy and Surface Vibrations*; Academic: New York, 1982.
(22) Enomoto, S.; Asahina, M. *J. Mol. Spectry.* **1966**, *19*, 117.
(23) Mizushima, S. *Structure of Molecules and Internal Rotation*; Academic: New York, 1954.
(24) Shimanouchi, T. *Tables of Molecular Vibrational Frequencies Consolidated Volume I*; National Bureau of Standards, 1972; pp 1−160.
(25) Herzberg, G. *Molecular Spectra and Molecular Structure, Vol. 2, Infrared and Raman Spectra of Polyatomic Molecules*; Van Nostrand Reinhold: New York, 1945.
(26) Schmidt, J.; Stuhlmann, C.; Ibach, H. *Surf. Sci.* **1994**, *302*, 10.
(27) Gao, Q.; Cheng, C. C.; Chen, P. J.; Choyke, W. J.; Yates, J. T., Jr. *J. Chem. Phys.* **1993**, *98*, 8308.
(28) Yoshinobu, J.; Tsuda, H.; Onchi, M.; Nishijima, M. *Solid State Commun.* **1986**, *60*, 801.
(29) *Eight Peak Index of Mass Spectra*; Mass Spectrometry Data Center, Aldermaston, 1974; Vol. 1.
(30) Coon, P. A.; Gupta, P.; Wise, M. L.; George, S. M. *J. Vac. Sci. Technol. A* **1992**, *10*, 324.
(31) Koleske, D. D.; Gates, S. M.; Beach, D. B. *J. Appl. Phys.* **1992**, *72*, 4073.
(32) Junker, K. H.; Hess, G.; Eherdt, J. G.; White, J. M. *J. Vac. Sci. Technol. A* **1998**, *16*, 2995.
(33) Oura, K.; Lifshits, V. G.; Saranin, A. A.; Zotov, A. V.; Katayama, M. *Surf. Sci. Rep.* **1999**, *35*, 1.
(34) Wallace, R. M.; Taylor, P. A.; Choyke, W. J.; Yates, J. T. *Surf. Sci.* **1990**, *239*, 1.
(35) Taylor, P. A.; Wallace, R. M.; Cheng, C. C.; Weinberg, W. H.; Dresser, M. J.; Choyke, W. J.; Yates, J. T., Jr. *J. Am. Chem. Soc.* **1992**, *114*, 6754.
(36) Lide, D. R. *CRC Handbook of Chemistry and Physics*, 85th ed.; CRC Press: Boca Raton, 2005.
(37) Cao, P.-L.; Zhou, R. J. *Phys. Condens. Matter* **1993**, *5*, 2887.
(38) Nishijima, M.; Yoshinobu, J.; Tsuda, H.; Onchi, M. *Surf. Sci.* **1987**, *192*, 383.
(39) Yoshinobu, J.; Tsuda, H.; Onchi, M.; Nishijima, M. *Chem. Phys. Lett.* **1986**, *130*, 170.
(40) He, Z. H.; Leung, K. T. *Surf. Sci.* **2005**, *583*, 179.
(41) Brown, W. A.; Kose, R.; King, D. A. *Chem. Rev.* **1998**, *98*, 797.
(42) Brown, W. A.; Kose, R.; King, D. A. *Surf. Sci.* **1999**, *440*, 271.
(43) Wang, Z. H.; Cao, Y.; Xu, G. Q. *Chem. Phys. Lett.* **2001**, *338*, 7.
(44) Foresman, J. B.; Frisch, Æ. *Exploring Chemistry with Electronic Structure Methods*, 2nd ed.; Gaussian Inc., Pittsburgh, 1996; and references therein.
(45) Frisch, M. J.; Trucks, G. W.; Schlegel, H. B.; Scuseria, G. E.; Robb, M. A.; Cheeseman, J. R.; Montgomery, J. A., Jr.; Vreven, T.; Kudin, K. N.; Burant, J. C.; Millam, J. M.; Iyengar, S. S.; Tomasi, J.; Barone, V.; Mennucci, B.; Cossi, M.; Scalmani, G.; Rega, N.; Petersson, G. A.; Nakatsuji, H.; Hada, M.; Ehara, M.; Toyota, K.; Fukuda, R.; Hasegawa, J.; Ishida, M.; Nakajima, T.; Honda, Y.; Kitao, O.; Nakai, H.; Klene, M.; Li, X.; Knox, J. E.; Hratchian, H. P.; Cross, J. B.; Adamo, C.; Jaramillo, J.; Gomperts, R.; Stratmann, R. E.; Yazyev, O.; Austin, A. J.; Cammi, R.; Pomelli, C.; Ochterski, J. W.; Ayala, P. Y.; Morokuma, K.; Voth, G. A.; Salvador, P.; Dannenberg, J. J.; Zakrzewski, V. G.; Dapprich, S.; Daniels, A. D.; Strain, M. C.; Farkas, O.; Malick, D. K.; Rabuck, A. D.; Raghavachari, K.; Foresman, J. B.; Ortiz, J. V.; Cui, Q.; Baboul, A. G.; Clifford, S.; Cioslowski, J.; Stefanov, B. B.; Liu, G.; Liashenko, A.; Piskorz, P.; Komaromi, I.; Martin, R. L.; Fox, D. J.; Keith, T.; Al-Laham, M. A.; Peng, C. Y.; Nanayakkara, A.; Challacombe, M.; Gill, P. M. W.; Johnson, B.; Chen, W.; Wong, M. W.; Gonzalez, C.; Pople, J. A. *Gaussian 03*, revision B.04; Gaussian, Inc., Pittsburgh, PA, 2003.
(46) Tong, S. Y.; Huang, H.; Wei, C. M.; Packard, W. E.; Men, F. K.; Glander, G.; Webb, M. B. *J. Vac. Sci. Technol. A* **1988**, *6*, 615.
(47) Petsalakis, I. D.; Polanyi, J. C.; Theodorakopoulos, G. *Surf. Sci.* **2003**, *544*, 162.
(48) Huheey, J. E. *Inorganic Chemistry*, 3rd ed.; Harper and Row: New York 1983.
(49) Huang, C.; Widdra, W.; Wang, X. S.; Weinberg, W. H. *J. Vac. Sci. Technol. A* **1993**, *11*, 2250 and references therein.
(50) Sanderson, R. T. *Polar Covalence*; Academic: New York, 1983.
(51) Sanderson, R. T. Chemical Bonds and Bond Energy, 2nd ed.; Academic: New York, 1976.